OPEN ACCESS Freely available online

PLOS ONE

Mathematical Modeling of Interleukin-27 Induction of Anti-Tumor T Cells Response

Kang-Ling Liao[1]*, Xue-Feng Bai[2], Avner Friedman[1,3]

1 Mathematical Biosciences Institute, The Ohio State University, Columbus, Ohio, United States of America, **2** Department of Pathology and Comprehensive Cancer Center, The Ohio State University, Columbus, Ohio, United States of America, **3** Department of Mathematics, The Ohio State University, Columbus, Ohio, United States of America

Abstract

Interleukin-12 is a pro-inflammatory cytokine which promotes Th1 and cytotoxic T lymphocyte activities, such as Interferon-γ secretion. For this reason Interleukin-12 could be a powerful therapeutic agent for cancer treatment. However, Interleukin-12 is also excessively toxic. Interleukin-27 is an immunoregulatory cytokine from the Interleukin-12 family, but it is not as toxic as Interleukin-12. In recent years, Interleukin-27 has been considered as a potential anti-tumor agent. Recent experiments *in vitro* and *in vivo* have shown that cancer cells transfected with IL-27 activate $CD8^+$ T cells to promote the secretion of anti-tumor cytokines Interleukin-10, although, at the same time, IL-27 inhibits the secretion of Interferon-γ by $CD8^+$ T cells. In the present paper we develop a mathematical model based on these experimental results. The model involves a dynamic network which includes tumor cells, $CD8^+$ T cells and cytokines Interleukin-27, Interleukin-10 and Interferon-γ. Simulations of the model show how Interleukin-27 promotes $CD8^+$ T cells to secrete Interleukin-10 to inhibit tumor growth. On the other hand Interleukin-27 inhibits the secretion of Interferon-γ by $CD8^+$ T cells which somewhat diminishes the inhibition of tumor growth. Our numerical results are in qualitative agreement with experimental data. We use the model to design protocols of IL-27 injections for the treatment of cancer and find that, for some special types of cancer, with a fixed total amount of drug, within a certain range, continuous injection has better efficacy than intermittent injections in reducing the tumor load while the treatment is ongoing, although the decrease in tumor load is only temporary.

Citation: Liao K-L, Bai X-F, Friedman A (2014) Mathematical Modeling of Interleukin-27 Induction of Anti-Tumor T Cells Response. PLoS ONE 9(3): e91844. doi:10.1371/journal.pone.0091844

Editor: Timothy W. Secomb, University of Arizona, United States of America

Received April 9, 2013; **Accepted** February 17, 2014; **Published** March 14, 2014

Funding: This work is supported, in part, by the National Science Council of Taiwan, R.O.C (http://web1.nsc.gov.tw/) under No. NSC 101-2917-I-564-062; the National Science Foundation (http://www.nsf.gov/) under Agreement DMS 0931642; the National Cancer Institute (http://www.cancer.gov/) under R01CA138427; and the American Cancer Society (http://www.cancer.org/) under RSG-09-188-01-LIB. The funders had no role in study design, data collection and analysis, decision to publish, or preparation of the manuscript.

Competing Interests: The authors have declared that no competing interests exist.

* E-mail: liao.92@mbi.osu.edu

Introduction

Interleukin-12 (IL-12) is a pro-inflammatory cytokine that plays a central role in the connection of the innate resistance and adaptive immunity, by promoting Th1 and cytotoxic T lymphocyte (CTL) activities, such as IFN-γ secretion. IL-12 could be a powerful therapeutic agent to eradicate tumor or to prevent the development of metastasis [1–4]. However, IL-12 has also been shown to be excessively toxic [5,6], although there is at least one ongoing clinical trial with IL-12 using a new delivery method (IL-12 DNA plasmid) that is intended to overcome toxicity problems. In recent years there has been increasing interest to investigate the role of another member of the IL-12 family, namely, Interleukin-27 (IL-27), which is less toxic than IL-12, as a potential anti-tumor agent [7]. IL-27 is a cytokine capable of regulating Th1, Th2, Th17, and T_{reg} responses [8]. In autoimmune diseases, Murugaiyan et al. [9] have shown that IL-27 promotes production of IL-10 and IFN-γ by naive human $CD4^+$ T cells, and Stumhofer et al. [10] demonstrated that IL-27 promotes production of IL-10 by $CD4^+$ and $CD8^+$ T cells. Reviewing the role of IL-27 in anti-cancer immunotherapy, Swarbrick et al. [11] asserted that IL-27 may have both pro-inflammatory and anti-inflammatory functions, and it promotes Th1 immune response and $CD8^+$ cell activation. Since Hisada et al. [7] first reported the anti-tumor efficacy of IL-27 in 2004, the potent anti-tumor activity of IL-27 has been verified in various tumor models [11–13]. Many studies suggest a role of IL-27 in enhancing anti-tumor $CD8^+$ T cell responses [7,14–17]. The enhancing role of IL-27 in generating anti-tumor CTL response was also demonstrated using IL-27R deficient mice [18,19].

IL-10 has inhibitory and stimulatory effects on human $CD8^+$ T cells [20], and in viral infection it is known to inhibit effector and memory $CD4^+$ T cell responses but not memory $CD8^+$ T cells [21]. IL-10 may have positive or negative effect on tumor suppression (Asadullah et al. [22]). Numerous studies (e.g. [23,24]) show that increase in IL-10 produced by macrophages is associated with tumor progression, while other studies [25–28] suggest that IL-10 plays a positive role in tumor rejection. IL-27 can induce production of IL-10 in $CD8^+$ T cells [10,29]. In a recent study, Liu et al. [30] used P1CTL TCR transgenic mouse model and mouse plasmacytoma tumor system to investigate how IL-27 enhances the anti-tumor responses. They found that IL-27 significantly enhances the survival of activated tumor antigen specific $CD8^+$ T cells *in vitro* and *in vivo*, and induces IL-10 upregulation in these T cells. It was also suggested in [30], and

demonstrated in [25–28], that CTL IL-10 production contributes to tumor rejection. These results have important implications for designing IL-27-based immunotherapy against human cancer.

In the present paper, we develop a mathematical model that describes the anti-tumor activity of $CD8^+$ T cells in terms of IFN-γ and IL-10 productions, when these T cells are activated by IL-27 from the tumor microenvironment. The model is based on the experiments by Liu et al. [30] (with mice infected with plasmacytoma) whereby cancer cells are transfected with an IL-27 vector so that IL-27 is released in the tumor microenvironment. We show that the model simulations agree qualitatively with the experimental results of [30]. We next extend the model to include therapeutic treatment of cancer in wild type mice by injection of IL-27. We note however, that in this case, the tumor microenvironment includes both $CD4^+$ and $CD8^+$ T cells (whereas in the experiments with transgenic mice of [30] the $CD8^+$ T cells were taken to be dominant). As mentioned above, IL-27 promotes the secretion of IL-10 and IFN-γ by $CD4^+$ T cells [9–11], and we assume that these cytokines have the same effect on tumor rejection as those secreted by $CD8^+$ T cells. We then use $CD8^+$ T cells to represent both cells, $CD4^+$ and $CD8^+$. In the modified model the only source of IL-27 comes from the drug, since cancer cells do not generally secrete IL-27. We compare the efficacy of different strategies of IL-27 injections. For example, we found that continuous injection of IL-27 for 24 weeks at a fixed amount F, within a certain range, is more effective than intermittent injection of the amount $2F$, full three weeks at a time with three weeks spacing between injections, for 24 weeks. These predictions however must be viewed just as suggestions since they may only apply to special types of cancer, such as plasmacytoma in bone or soft tissue, and since, furthermore, the model does not include other important factors in tumor progression such as angiogenesis and the immune response.

Results

Mathematical model

In this model, we assume that the tumor is spherical and that it initially lies in a spherical tissue of radius L. The variables that will be used in the model are listed below and we assume that all the variables are radially symmetric:

$$\begin{aligned} I_{27}(r,t) &: \text{concentration of Interleukin}-27 \text{ in } pg/cm^3,\\ I_{10}(r,t) &: \text{concentration of Interleukin}-10 \text{ in } pg/cm^3,\\ T(r,t) &: \text{(tumor antigen specific) activated } CD8^+ \text{ T cell density, } cell/cm^3,\\ I_\gamma(r,t) &: \text{concentration of Interferon}-\gamma \text{ in } pg/cm^3,\\ c(r,t) &: \text{tumor cell density, } cell/cm^3, \end{aligned}$$

where r is the distance from a point $x=(x_1,x_2,x_3)$ to the origin: $r=\sqrt{x_1^2+x_2^2+x_3^2}$ and $0\le r\le L$. These variables satisfy a system of

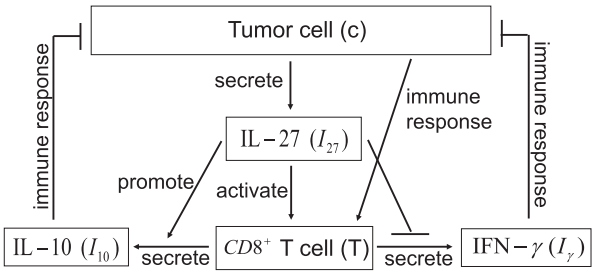

Figure 1. A network of IL-27. A network showing how IL-27 affects the immune response to tumor cells. $CD8^+$ T cells are activated by P1A antigen from tumor cells as well as by IL-27 which is secreted by tumor cells. Activated $CD8^+$ T cells secrete IFN-γ, inhibited by IL-27, and IL-10 enhanced by IL-27. IL-10 and IFN-γ inhibit tumor cells.
doi:10.1371/journal.pone.0091844.g001

partial differential equations based on the network exhibited in Figure 1. The parameter values are estimated in Methods. In our model we shall include diffusion of cells and cytokines, as was done in many other models of solid tumors (which include plasmacytoma [31–38])

IL-27. The following equation describes the evolution of I_{27}:

$$\frac{\partial I_{27}}{\partial t}=\underbrace{D_{I_{27}}\frac{1}{r^2}\frac{\partial}{\partial r}\left(r^2\frac{\partial I_{27}}{\partial r}\right)}_{\text{diffusion}}+\underbrace{\alpha_{27}c}_{\text{production by tumor}}-\underbrace{\mu_{27}I_{27}}_{\text{degradation}}. \quad (1)$$

The first term represents the diffusion of I_{27} with coefficient $D_{I_{27}}$. Although diffusivities of cytokines and cells may depend on the concentrations of the tumor cells and normal healthy cells, for simplicity, here and in the sequel all diffusivities are assumed to be spatially uniform. In the experiment in [30], Liu et al. used gene transfected tumor cells, J558-IL-27, to produce I_{27} in the tumor microenvironment. Accordingly, we use the second term to describe the production of I_{27} by the transfected J558-IL-27 tumor cells. The last term stands for the degradation of I_{27}. The parameter values of Equation (1) are given in Table 1.

IL-10. The Interleukin-10 (IL-10) in Figure 1 is pro-inflammatory, in accordance with the experiments of [30]. It satisfies the equation:

$$\begin{aligned}\frac{\partial I_{10}}{\partial t}=&\underbrace{D_{I_{10}}\frac{1}{r^2}\frac{\partial}{\partial r}\left(r^2\frac{\partial I_{10}}{\partial r}\right)}_{\text{diffusion}}+\underbrace{s_{10}T}_{\text{production by CTL without } I_{27}}\\&+\underbrace{\alpha_{10}T\frac{I_{27}}{I_{27}+\sigma_{10}}}_{\text{production by CTL promoted by } I_{27}}-\underbrace{\mu_{10}I_{10}}_{\text{degradation}}.\end{aligned} \quad (2)$$

Table 1. Parameters for the IL-27 equation.

Parameter	Description	Value with unit	Reference
$D_{I_{27}}$	diffusion coefficient of I_{27}	$1.25\times10^{-3}cm^2/day$	[48] & estimated
α_{27}	production rate of I_{27} from tumor	$1.5\times10^{-5}pg/cell/day$	[30] & estimated
μ_{27}	degradation rate of I_{27}	$2/day$	[48] & estimated

doi:10.1371/journal.pone.0091844.t001

Table 2. Parameters for the IL-10 equation.

Parameter	Description	Value with unit	Reference
$D_{I_{10}}$	diffusion coefficient of I_{10}	$1.25\times10^{-3}cm^2/day$	[48]
s_{10}	production rate from CTL without IL-27	$8.89\times10^{-8}pg/cell/day$	[30] & estimated
α_{10}	max production rate from CTL with IL-27	$1.128\times10^{-4}pg/cell/day$	[30] & estimated
σ_{10}		$5\times10^{3}pg/cm^3$	[49] & estimated
μ_{10}	degradation rate of I_{10}	$1.6\times10/day$	[48]

doi:10.1371/journal.pone.0091844.t002

The first term is the diffusion of I_{10}. The second term accounts for the production of I_{10} by $CD8^+$ T cells for the absence of I_{27} [30]. The experiments in [30] indicate that I_{27} significantly increases the production of I_{10} by $CD8^+$ T cells, and this is accounted by the third term. The last term is the degradation of I_{10}. The parameter values of Equation (2) are listed in Table 2.

$CD8^+$ T cells. The equation for the density of (activated) $CD8^+$ T cells, $T(x,t)$, is given by

$$\frac{\partial T}{\partial t}=\underbrace{D_T\frac{1}{r^2}\frac{\partial}{\partial r}(r^2\frac{\partial T}{\partial r})}_{\text{diffusion}}+\underbrace{s_T\frac{c}{c+c_T}}_{\text{immune response}}-\underbrace{\frac{\mu_T}{1+\sigma_T I_{27}+\beta_T\sigma_T I_{10}}T}_{\text{pro-survival by } I_{27} \text{ and } I_{10}}. \quad (3)$$

The first term is a dispersion of $CD8^+$ T cells with coefficient D_T. The second term accounts for activation of $CD8^+$ T cells by P1A antigen from the tumor cells. I_{27} promotes survival of $CD8^+$ T cells, and so does also I_{10}, but to a smaller degree [30]. We present these two facts by correspondingly decreasing the death rate μ_T of T cells in the last term of Equation (3). The parameter values in Equation (3) are given in Table 3. Although I_{27} contributes more than I_{10} to promote the half-life of $CD8^+$ T cells, we take $\beta_T=9$ since the concentration of I_{10} is much smaller than the concentration of I_{27}.

IFN-γ. Interferon-γ (IFN-γ) is a cytokine with diffusion coefficient D_γ and degradation rate μ_γ. It is produced by T cells and, as shown in [30], the production is inhibited by I_{27}. Thus, $I_\gamma(x,t)$ satisfies the equation:

$$\frac{\partial I_\gamma}{\partial t}=\underbrace{D_\gamma\frac{1}{r^2}\frac{\partial}{\partial r}(r^2\frac{\partial I_\gamma}{\partial r})}_{\text{diffusion}}+\underbrace{\alpha_\gamma T\frac{s_\gamma}{s_\gamma+I_{27}}}_{\text{production by CTL inhibited by } I_{27}}-\underbrace{\mu_\gamma I_\gamma}_{\text{degradation}}. \quad (4)$$

Table 4 lists all parameter values of (4).

Tumor cells. The density of tumor cells, $c(x,t)$, satisfies the following equation:

$$\frac{\partial c}{\partial t}=\underbrace{D_c\frac{1}{r^2}\frac{\partial}{\partial r}(r^2\frac{\partial c}{\partial r})}_{\text{diffusion}}+\underbrace{\lambda_1 c(1-\frac{c}{c_*})}_{\text{proliferation}}-\underbrace{\mu_c c}_{\text{death}}-\underbrace{\eta_c\frac{I_{10}}{I_{10}+\sigma_c}c}_{\text{inhibition by } I_{10}}-\underbrace{\eta_\gamma\frac{I_\gamma}{I_\gamma+s_c}c}_{\text{inhibition by IFN}-\gamma}. \quad (5)$$

The second and third terms represent the proliferation and death of cells, respectively. Generally, I_{10} is regarded as an anti-inflammatory cytokine. However, in different experimental models, I_{10} could suppress or promote the functions of immune system [30,39]. Liu et al. [30] found that the I_{10} produced by CTL contributes to tumor rejection. Hence, the fourth term accounts for the indirect inhibition of tumor cells by I_{10}. Cytokine, I_γ promotes the anti-tumor response, such as increase production of IL-12, and induces natural killer cells to kill cancer cells [40,41]. For simplicity, we take the fifth term in (5) to represent the

Table 3. Parameters for $CD8^+$ T cell equation.

Parameter	Description	Value with unit	Reference
D_T	diffusion coefficient of CTL	$4.32\times10^{-6}cm^2/day$	[48]
s_T	production rate of CTL activated by tumor	$1.3968\times10^{8}cell/cm^3/day$	[30] & estimated
c_T		$5.76\times10^{10}cell/cm^3$	estimated
σ_T		$2\times10^{-4}pg/cm^3$	estimated
β_T		9	estimated
μ_T	death rate of CTL	$3\times10^{-1}/day$	[48]

doi:10.1371/journal.pone.0091844.t003

Table 4. Parameters for the IFN-γ equation.

Parameter	Description	Value with unit	Reference
D_γ	diffusion coefficient of I_γ	$1.25\times10^{-3}cm^2/day$	[48] & estimated
α_γ	max production rate of I_γ from CTL	$3.72\times10^{-5}pg/cell/day$	[30] & estimated
s_γ		$5\times10^{6}pg/cm^3$	estimated
μ_γ	degradation rate of I_γ	$2.16/day$	[49]

doi:10.1371/journal.pone.0091844.t004

(indirect) inhibition of tumor cells by I_γ. The parameter values are listed in Table 5.

The dimensional and dimensionless values of all the parameters of Tables 1–5 are listed in Table 6.

Initial conditions. We assume that tumor cells are initially concentrated near $r=0$, taking

$$c(r,0)=c_0(e^{-r/\epsilon}-e^{-L/\epsilon}),\ \text{where L}=1\ \text{cm or L}=1.5\ \text{cm},$$

and ϵ is a positive number less than or equal to 1. In the simulations, we shall take $\epsilon=1$ but the results do not change qualitatively with smaller values of ϵ. Since I_{27} is produced by J558-IL-27 tumor cells, the initial concentration of I_{27} should be similar to the density of tumor cells; we take

$$I_{27}(r,0)=\frac{\alpha_{27}}{\mu_{27}}c_0(e^{-r/\epsilon}-e^{-L/\epsilon}).$$

Initially, there are no activated $CD8^+$ T cells, hence

$$T(r,0)=0.$$

Since I_{10} and I_γ are produced by $CD8^+$ T cells, we take

$$I_{10}(r,0)=0\ \text{and}\ I_\gamma(r,0)=0.$$

Boundary conditions. Since all variables are radially symmetric, the first r-derivative at $r=0$ is equal to zero. We assume no-flux condition for all variables at $r=L$. This is justified by the fact that L is large enough so that the exterior of the ball of radius L lies completely within the healthy tissue, initially.

Parameters nondimensionalization. We nondimensionalizate the Equations (1) – (5):

$$\hat{r}=r/L_0,\hat{t}=t/\tau,$$

$$\hat{I}_{27}=I_{27}/I_{27}^0,\hat{I}_{10}=I_{10}/I_{10}^0,\hat{T}=T/T^0,\hat{I}_\gamma=I_\gamma/I_\gamma^0,\hat{c}=c/c_0,$$

$$\{\hat{D}_{I_{27}},\hat{D}_{I_{10}},\hat{D}_T,\hat{D}_\gamma,\hat{D}_c\}=\frac{\tau}{L_0^2}\{D_{I_{27}},D_{I_{10}},D_T,D_\gamma,D_c\},$$

$$\{\hat{\alpha}_{27},\hat{\alpha}_{10},\hat{\alpha}_\gamma\}=\tau\{c_0\alpha_{27}/I_{27}^0,T_0\alpha_{10}/I_{10}^0,T_0\alpha_\gamma/I_\gamma^0\},$$

$$\{\hat{\mu}_{27},\hat{\mu}_{10},\hat{\mu}_T,\hat{\mu}_\gamma,\hat{\mu}_c\}=\tau\{\mu_{27},\mu_{10},\mu_T,\mu_\gamma,\mu_c\},$$

$$\{\hat{s}_{10},\hat{s}_T\}=\tau\{T_0s_{10}/I_{10}^0,s_T/T_0\},\{\hat{\eta}_c,\hat{\eta}_\gamma\}=\tau\{\eta_c,\eta_\gamma\},$$

$$\{\hat{\sigma}_{10},\hat{s}_\gamma\}=\frac{1}{I_{27}^0}\{\sigma_{10},s_\gamma\},\hat{\sigma}_T=I_{27}^0\sigma_T,\hat{\beta}_T=\beta_T,$$

$$\hat{\sigma}_c=\sigma_c/I_{10}^0,\hat{s}_c=s_c/I_\gamma^0,\hat{\lambda}_1=\tau\lambda_1,\hat{c}_*=c_*/c_0,\hat{c}_T=c_T/c_0,$$

where

$$\tau=3\ days,\ L_0=0.5\ cm$$

Table 5. Parameters for tumor cell equation.

Parameter	Description	Value with unit	Reference
D_c	diffusion coefficient of tumor	$8.64\times10^{-6}cm^2/day$	[48]
λ_1	max proliferation rate	$4.68\times10^{-1}/day$	[30] & estimated
c_*		$10^9cell/cm^3$	[48]
μ_c	death rate of tumor	$1.73\times10^{-1}/day$	[48] & estimated
η_c	inhibition rate of tumor from I_{10}	$3.45\times10^{-1}/day$	[30] & estimated
σ_c		$1.5\times10^{2}pg/cm^3$	estimated
η_γ	inhibition rate of tumor from IFN-γ	$6\times10^{-1}/day$	[30] & estimated
s_c		$3\times10^{2}pg/cm^3$	estimated

doi:10.1371/journal.pone.0091844.t005

Table 6. Model variables and units.

Parameter	Dimension value	Dimensionless value
$D_{I_{27}}$	$1.25\times10^{-3}cm^2/day$	1.5×10^{-2}
$D_{I_{10}}$	$1.25\times10^{-3}cm^2/day$	1.5×10^{-2}
D_T	$4.32\times10^{-6}cm^2/day$	5.184×10^{-5}
D_γ	$1.25\times10^{-3}cm^2/day$	1.5×10^{-2}
D_c	$8.64\times10^{-6}cm^2/day$	1.0368×10^{-4}
μ_{27}	$2/day$	6
μ_{10}	$1.6\times10/day$	4.8×10
μ_T	$3\times10^{-1}/day$	9×10^{-1}
μ_γ	$2.16/day$	6.48
μ_c	$1.73\times10^{-1}/day$	5.19×10^{-1}
α_{27}	$1.5\times10^{-5}pg/cell/day$ for small production	3.24×10^2
	$7.5\times10^{-5}pg/cell/day$ for moderate production	$3.24\times10^2\times5$
	$3\times10^{-4}pg/cell/day$ for large production	$3.24\times10^2\times20$
α_{10}	$1.128\times10^{-4}pg/cell/day$	3.384×10^{-1}
α_γ	$3.72\times10^{-5}pg/cell/day$	1.116×10^{-1}
β_T	9	9
s_{10}	$8.89\times10^{-8}pg/cell/day$	2.667×10^{-4}
s_T	$1.3968\times10^8cell/cm^3/day$	4.1904×10^3
s_γ	$5\times10^6pg/cm^3$	5×10^4
s_c	$3\times10^2pg/cm^3$	3
σ_{10}	$5\times10^3pg/cm^3$	5×10
σ_T	$2\times10^{-4}pg/cm^3$	2×10^{-2}
σ_c	$1.5\times10^2pg/cm^3$	1.5
η_c	$3.45\times10^{-1}/day$	1.035
η_γ	$6\times10^{-1}/day$	1.8
λ_1	$4.68\times10^{-1}/day$	1.404
c_*	$10^9cell/cm^3$	1.38889
c_T	$5.76\times10^{10}cell/cm^3$	8×10
L	$1cm$ in Figs. 2–5	2
	$1.5cm$ in Figs. 6–10	3
τ	$3days$	1
L_0	$5\times10^{-1}cm$	1
c_0	$7.2\times10^8cell/cm^3$	1
T_0	$10^5cell/cm^3$	1
I_{27}^0	$10^2pg/cm^3$	1
I_{10}^0	$10^2pg/cm^3$	1
I_γ^0	$10^2pg/cm^3$	1
F	$3\times10^4pg/cm^3/day$ in Figs. 6, 7, and 10	9×10^2
	$1\times10^4pg/cm^3/day$ in Figs. 8A and 9A	3×10^2
	$0.5\times10^4pg/cm^3/day$ in Figs. 8B and 9B	1.5×10^2
a	$2.25cm^2$	9

doi:10.1371/journal.pone.0091844.t006

$$c_0=7.2\times10^8cell/cm^3,\ T_0=10^5cell/cm^3$$

$$I_{27}^0=I_{10}^0=I_\gamma^0=10^2pg/cm^3.$$

For nondimensional variables and parameters, we consider the tumor growth in a ball $\{\hat r\le2\}$ or $\{\hat r\le3\}$. The nondimensional PDE model is given by the following system of equations:

$$\begin{cases}
\dfrac{\partial\hat I_{27}}{\partial\hat t} &= \underbrace{\hat D_{I_{27}}\dfrac{1}{\hat r^2}\dfrac{\partial}{\partial\hat r}\left(\hat r^2\dfrac{\partial\hat I_{27}}{\partial\hat r}\right)}_{\text{diffusion}}+\underbrace{\hat\alpha_{27}\hat c}_{\text{production by tumor}}-\underbrace{\hat\mu_{27}\hat I_{27}}_{\text{degradation}}\\
\dfrac{\partial\hat I_{10}}{\partial\hat t} &= \underbrace{\hat D_{I_{10}}\dfrac{1}{\hat r^2}\dfrac{\partial}{\partial\hat r}\left(\hat r^2\dfrac{\partial\hat I_{10}}{\partial\hat r}\right)}_{\text{diffusion}}+\underbrace{\hat s_{10}\hat T}_{\text{production by CTL without }\hat I_{27}}\\
&\quad+\underbrace{\hat\alpha_{10}\hat T\dfrac{\hat I_{27}}{\hat I_{27}+\hat\sigma_{10}}}_{\text{production by CTL promoted by }\hat I_{27}}-\underbrace{\hat\mu_{10}\hat I_{10}}_{\text{degradation}}\\
\dfrac{\partial\hat T}{\partial\hat t} &= \underbrace{\hat D_T\dfrac{1}{\hat r^2}\dfrac{\partial}{\partial\hat r}\left(\hat r^2\dfrac{\partial\hat T}{\partial\hat r}\right)}_{\text{diffusion}}+\underbrace{\hat s_T\dfrac{\hat c}{\hat c+\hat c_T}}_{\text{immune response}}\\
&\quad-\underbrace{\dfrac{\hat\mu_T}{1+\hat\sigma_T\hat I_{27}+\hat\beta_T\hat\sigma_T\hat I_{10}}\hat T}_{\text{pro-survival by }I_{27}\text{ and }I_{10}}\\
\dfrac{\partial\hat I_\gamma}{\partial\hat t} &= \underbrace{\hat D_\gamma\dfrac{1}{\hat r^2}\dfrac{\partial}{\partial\hat r}\left(\hat r^2\dfrac{\partial\hat I_\gamma}{\partial\hat r}\right)}_{\text{diffusion}}+\underbrace{\hat\alpha_\gamma\hat T\dfrac{\hat s_\gamma}{\hat s_\gamma+\hat I_{27}}}_{\text{production by CTL inhibited by }\hat I_{27}}\\
&\quad-\underbrace{\hat\mu_\gamma\hat I_\gamma}_{\text{degradation}}\\
\dfrac{\partial\hat c}{\partial\hat t} &= \underbrace{\hat D_c\dfrac{1}{\hat r^2}\dfrac{\partial}{\partial\hat r}\left(\hat r^2\dfrac{\partial\hat c}{\partial\hat r}\right)}_{\text{diffusion}}+\underbrace{\hat\lambda_1\hat c\left(1-\dfrac{\hat c}{\hat c_*}\right)}_{\text{proliferation}}-\underbrace{\hat\mu_c\hat c}_{\text{death}}\\
&\quad-\underbrace{\hat\eta_c\dfrac{\hat I_{10}}{\hat I_{10}+\hat\sigma_c}\hat c}_{\text{inhibition by }\hat I_{10}}-\underbrace{\hat\eta_\gamma\dfrac{\hat I_\gamma}{\hat I_\gamma+\hat s_c}\hat c}_{\text{inhibition by IFN}-\gamma}.
\end{cases}\tag{6}$$

Numerical simulation

The model (6) was simulated, in nondimensional variables, using matlab with $d\hat r=0.02$ and $d\hat t=0.01$ (i.e., $dr=0.01cm$ and $dt=\frac{3}{100}day$ in dimensional units). Four cases were considered:

(i) J558-Ctrl tumor cells.

(ii) J558-IL-27 tumor cells with small production rate of IL-27.

(iii) J558-IL-27 tumor cells with moderate production rate of IL-27.

(iv) J558-IL-27 tumor cells with large production rate of IL-27.

It has been reported in [30] that I_{27} can enhance the population of CD8$^+$ T cells. Moreover, I_{27} also enhances I_{10} produced by CD8$^+$ T cells to inhibit the tumor growth, but at the same time it suppresses the pro-inflammatory cytokine I_γ secreted by CD8$^+$ T cells. In spite of its inhibition of I_γ, I_{27} still promotes CD8$^+$ T cells to suppress the tumor growth.

In view of these experimental results we expect the total mass of I_{10} to increase from cases (i) to (iv), the total CD8$^+$ T cell population to increase from cases (i) to (iv), and the total population of cancer cells to decrease from cases (i) to (iv), as time progresses.

Correspondingly, we associate with the four cases (i) – (iv) increasing values of the parameter α_{27}:

$$\hat{\alpha}_{27} = 0 \text{ and } \hat{I}_{27}(\hat{r},0)=0,\hat{r}\in[0,2] \text{ in Figures. } 2-5, \text{ in case (i) of J558}-\text{Ctrl tumor cells},$$

$$\hat{\alpha}_{27} = 0 \text{ and } \hat{I}_{27}(\hat{r},0)=0,\hat{r}\in[0,3] \text{ in Figures. } 6-9, \text{ in case (i) of J558}-\text{Ctrl tumor cells},$$

$$\hat{\alpha}_{27} = 324(\text{i.e., } \alpha_{27}=1.5\times10^{-5}pg/cell/day), \text{ in case (ii)},$$

$$\hat{\alpha}_{27} = 324\times5(\text{i.e., } \alpha_{27}=7.5\times10^{-5}pg/cell/day), \text{ in case (iii)},$$

$$\hat{\alpha}_{27} = 324\times20(\text{i.e., } \alpha_{27}=3\times10^{-4}pg/cell/day), \text{ in case (iv)}.$$

In Figures 2-5, we took $L=1cm$ such that tumor cells are not visible near the boundary $r=1cm$ for all time $t\in[0,90days]$. Figure 2 shows the time-dependent profiles of the total mass of I_{27},I_{10},I_γ, and total populations of CD8$^+$ T cells and cancer cells. We see that growth/decrease of these variables, as $\hat{\alpha}_{27}$ varies, corresponds qualitatively to the experiments in [30]. Figures 3-5 show significant spatial variations of these variables at days 3,9, and 15, with or without production of I_{27}. We also see the effect of I_{27} on cancer cells and CD8$^+$ T cells densities at different distances from the point of origin of the cancer. For example, at the origin, at day 3 the cancer cells density changed from $4.95\times10^8 cell/cm^3$ with no treatment by I_{27} to $4.65\times10^8 cell/cm^3$ with largest production of I_{27}, while at day 15 it changed from $4.2\times10^8 cell/cm^3$ with no treatment to $1.7\times10^8 cell/cm^3$ with largest production of I_{27}. Similarly, at the origin, the CD8$^+$ T cell density increased at day 3 from $2.3\times10^6 cell/cm^3$ without treatment to $3.3\times10^6 cell/cm^3$ with largest production of I_{27}, whereas at day 15 the density increased even more significantly from $3.5\times10^6 cell/cm^3$ with no I_{27} treatment to $9\times10^6 cell/cm^3$ with maximal production of I_{27}. Note that Figure 5E and 5F show that the tumor cell density is almost zero near the boundary $r=1cm$ and the tumor cells concentrate in the region $r=0.5cm$.

Tumor initiating in internal organs can also be treated by I_{27}, but the mechanism for introducing I_{27} will depend on the location of the tumor. For example, in colitis induced colon cancer, one could use yeast which were programmed to express I_{27} [42]. Oncolytic virus which are engineered to produce I_{27} within tumor cells could turn the tumor into immunogenetic, thus enabling the immune system to reject the tumor.

We want to use our model in order to design treatments for a wild type mouse by I_{27} injection. We recall, as noted in the Introduction, that for wild type mouse, both CD4$^+$ and CD8$^+$ T

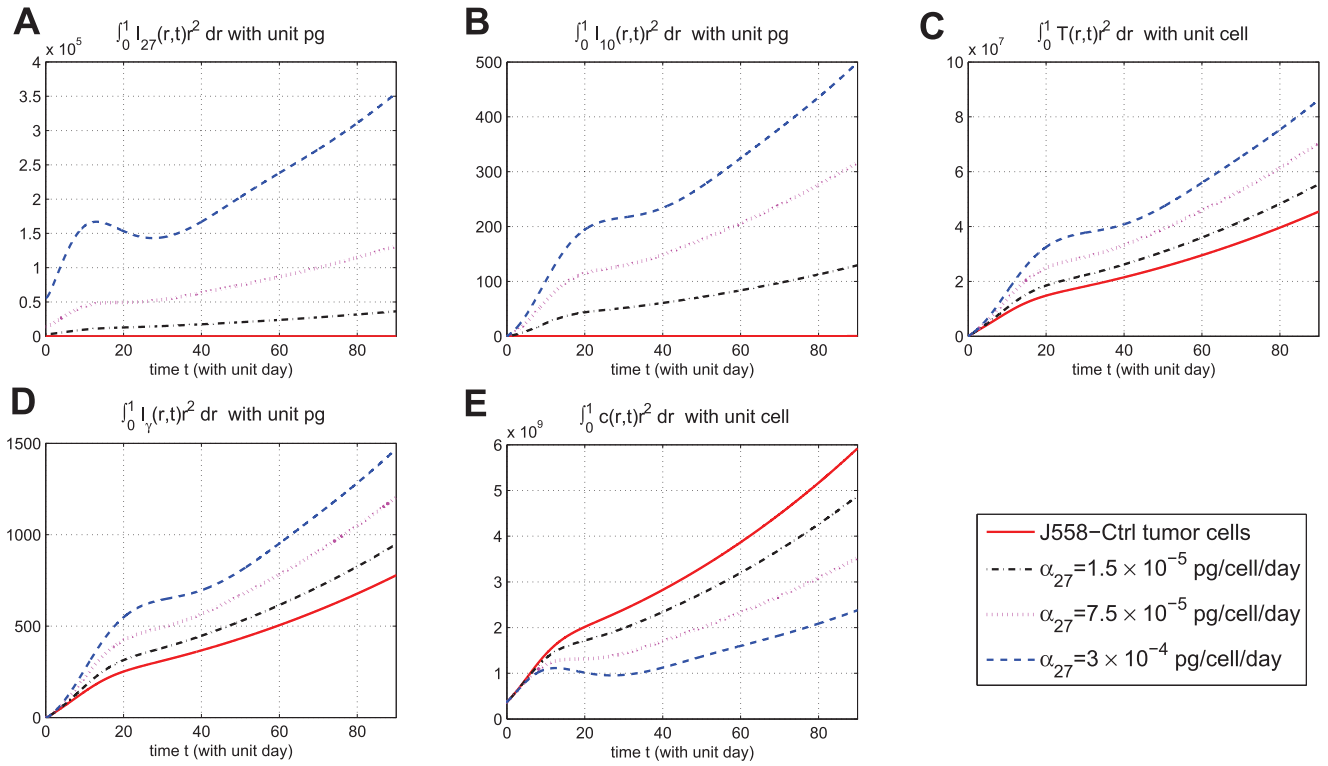

Figure 2. Evolution of cells and cytokines for different production rates of IL-27. (A), (B), (C), (D), and (E) are the profiles of total number of I_{27},I_{10},T,I_γ, and c, respectively, within 90 days. In (E), the curves displayed from top to bottom are for J558-Ctrl tumor cells, J558-IL-27 tumor cells with small ($\alpha_{27}=1.5\times10^{-5}pg/cell/day$), moderate ($\alpha_{27}=7.5\times10^{-5}pg/cell/day$), and large ($\alpha_{27}=3\times10^{-4}pg/cell/day$) production of IL-27, successively; $L=1cm$.
doi:10.1371/journal.pone.0091844.g002

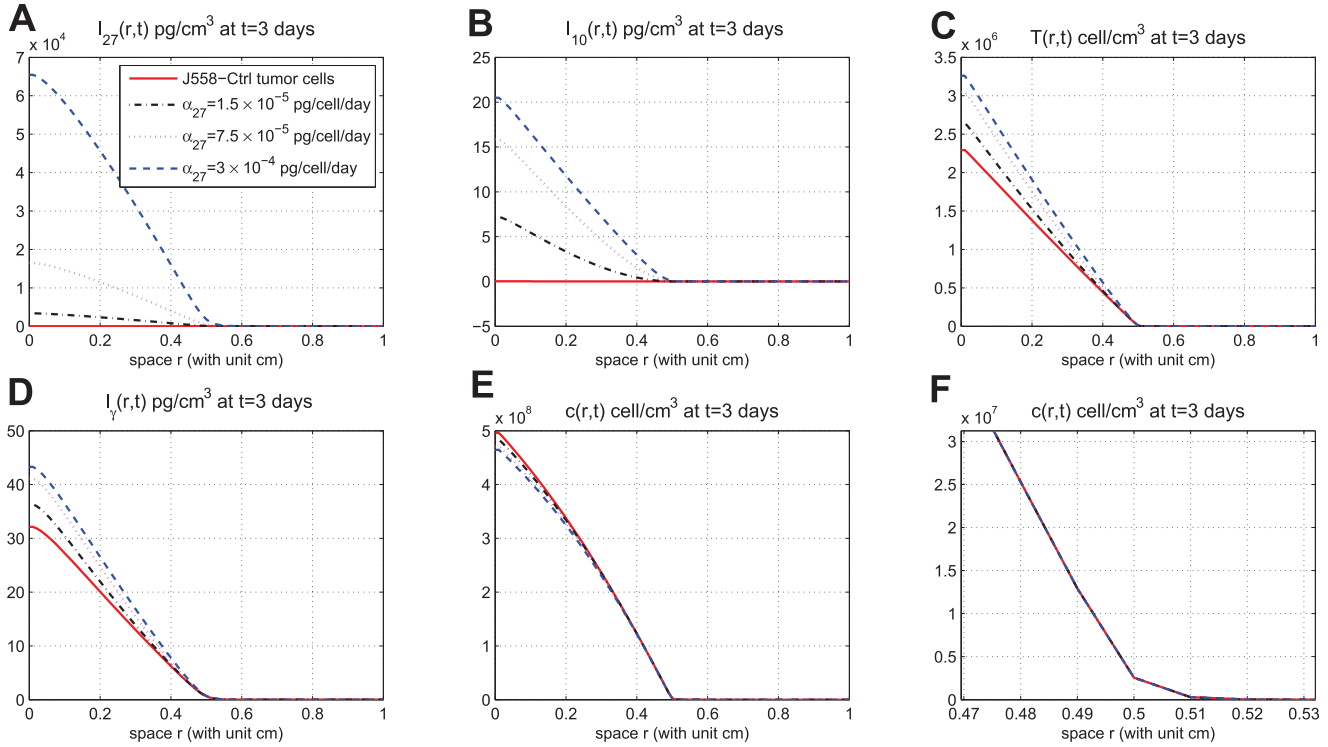

Figure 3. Spatial distributions at day 3. (A), (B), (C), (D), and (E) are the spatial distributions of $I_{27}, I_{10}, T, I_\gamma$, and c, respectively, at day 3 for different production rates of IL-27. (F) is zoomed in (E) near $r=0.5cm$. In (E), the curves displayed from top to bottom are for J558-Ctrl tumor cells, J558-IL-27 tumor cells with small ($\alpha_{27}=1.5\times10^{-5}pg/cell/day$), moderate ($\alpha_{27}=7.5\times10^{-5}pg/cell/day$), and large ($\alpha_{27}=3\times10^{-4}pg/cell/day$) production of IL-27, successively; $L=1cm$.
doi:10.1371/journal.pone.0091844.g003

cells produce IL-10 and IFN-γ [9–11] and we assume that IL-10 secreted by CD4$^+$ T cells has the same tumor rejection quality as the IL-10 secreted by CD8$^+$ T cells. We then use CD8$^+$ T cells to represent both cells, CD4$^+$ and CD8$^+$. We also note that *in vivo* tumor cells do not generally secrete I_{27}, so we take $\hat{\alpha}_{27}=0$ in Equation (1). But we also need to include an injection term in Equation (1) for I_{27}. If we denote the injection density by $f(r,t)$ then Equation (1) becomes

$$\frac{\partial I_{27}}{\partial t}=\underbrace{D_{I_{27}}\frac{1}{r^2}\frac{\partial}{\partial r}(r^2\frac{\partial I_{27}}{\partial r})}_{\text{diffusion}}+\underbrace{f(r,t)}_{\text{injection of } I_{27}}-\underbrace{\mu_{27}I_{27}}_{\text{degradation}}. \quad (7)$$

We make the pharmacokinetic assumption that $f(r,t)$ decreases in r from the outer boundary of the tumor ($r=1.5cm$) towards the inner core ($r=0$), and take

$$f(r,t)=F\times\frac{r^2+a}{L^2+a}, \quad (8)$$

where a is some positive constant; F is viewed as the "amount" of injection.

We consider here, for illustration, two strategies of treatment: (i) continuous injection of I_{27} at a fixed amount F for 24 weeks, and (ii) intermittent injections, at double amount $2F$, full three weeks at a time with three weeks spacing between injections. Accordingly, for the continuous strategy

$$f(r,t)=\begin{cases}F\times\frac{r^2+a}{L^2+a}, & \text{for } 0\le r\le L \text{ and } 0\le t\le 24 \text{ weeks (in real time)},\\ 0, & \text{for } 0\le r\le L \text{ and } 24<t\le 30 \text{ weeks (in real time)},\end{cases} \quad (9)$$

and for the intermittent strategy

$$f(r,t)=\begin{cases}2F\times\frac{r^2+a}{L^2+a}, & \text{for } 0\le r\le L \text{ and } t_{2i}\le t<t_{2i+1},\ i=0,1,2,3\\ 0, & \text{for } 0\le r\le L \text{ and } t_{2i+1}\le t<t_{2(i+1)},\ i=0,1,2,3 \text{ and } 24<t\le 30 \text{ weeks}\end{cases} \quad (10)$$

in case (ii), where the length of each interval $[t_j,t_{j+1}]$ is three weeks (the drug is injected only during the intermittent intervals $[t_{2i},t_{2i+1}]$) and $t_0=0$. In the following simulations, we take $a=2.25cm^2$; however the same results remain qualitatively the same for other values of a (not shown here).

In Figures 6-9, we take $L=1.5cm$ so that the tumor cell density remains negligible near the boundary $r=L$, during the entire simulation time which is 30 weeks and hence the boundary conditions are not affecting the results during the entire simulation (For longer simulation time, e.g. 60 weeks, we need to take $L=3cm$ (not shown here.)). We also take the simulation mesh size $dr=0.01cm$ and $dt=0.01day$. In Figure 6, we compare the results of the two strategies in case $F=3\times10^4pg/cm^3/day$. We see that continuous injection yields better results in reducing the tumor level and slightly delaying relapse after the drug is withdrawn.

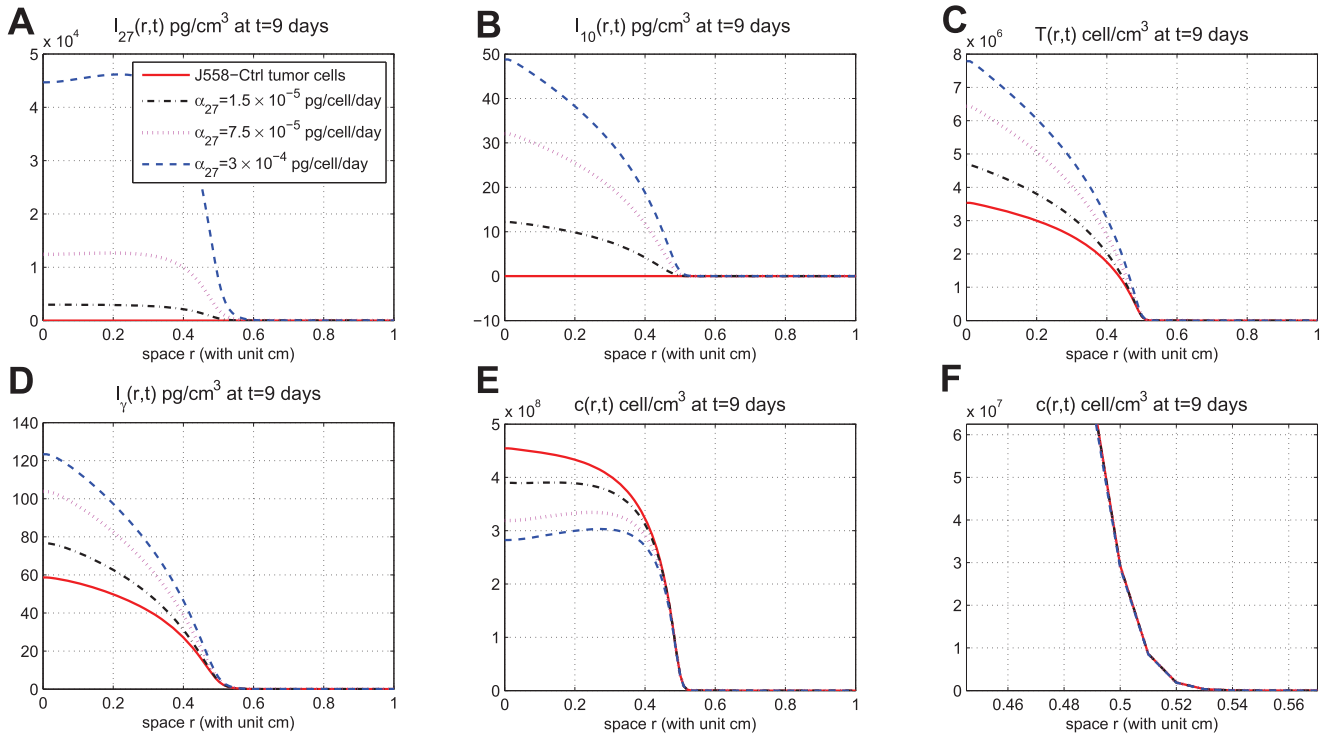

Figure 4. Spatial distributions at day 9. (A), (B), (C), (D), and (E) are the spatial distributions of $I_{27}, I_{10}, T, I_\gamma$, and c, respectively, at day 9 for different production rates of IL-27. (F) is zoomed in (E) near $r = 0.5cm$. In (E), the curves displayed from top to bottom are for J558-Ctrl tumor cells, J558-IL-27 tumor cells with small ($\alpha_{27} = 1.5 \times 10^{-5} pg/cell/day$), moderate ($\alpha_{27} = 7.5 \times 10^{-5} pg/cell/day$), and large ($\alpha_{27} = 3 \times 10^{-4} pg/cell/day$) production of IL-27, successively; $L = 1cm$.
doi:10.1371/journal.pone.0091844.g004

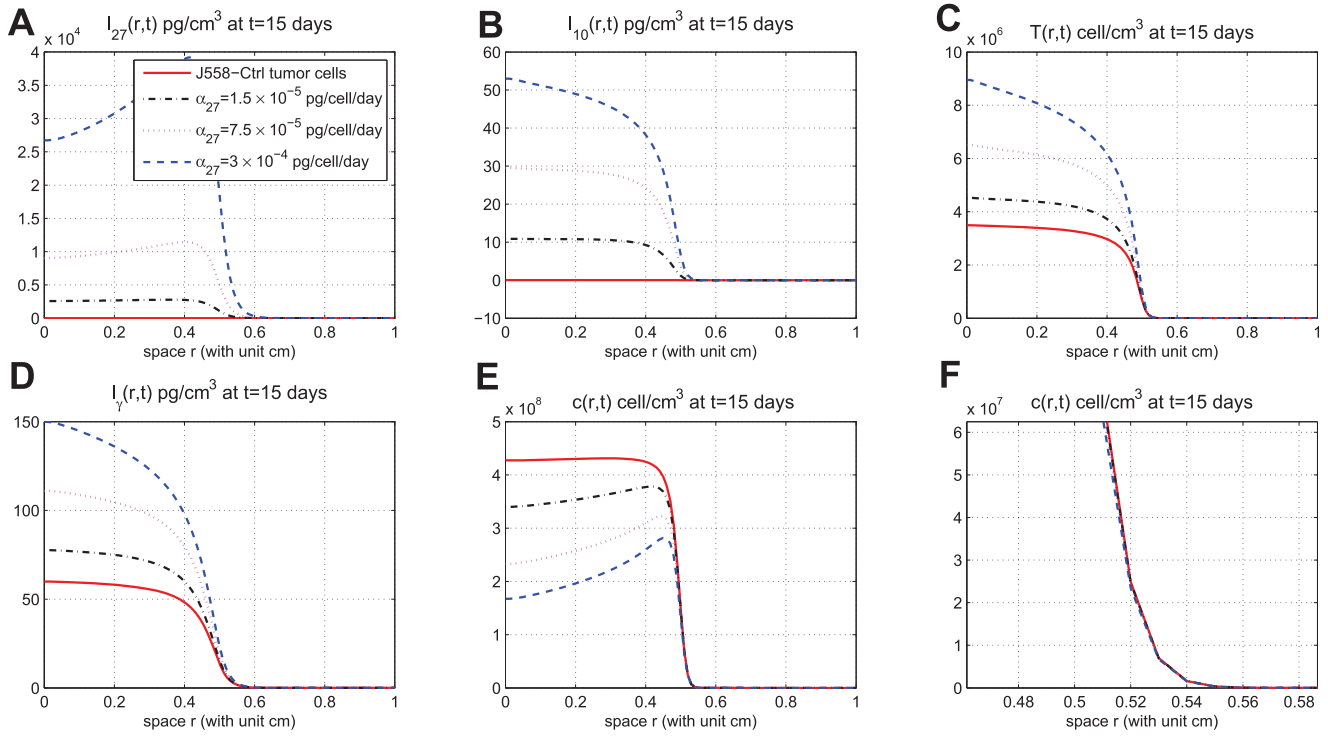

Figure 5. Spatial distributions at day 15. (A), (B), (C), (D), and (E) are the spatial distributions of $I_{27}, I_{10}, T, I_\gamma$, and c, respectively, at day 15 for different production rates of IL-27. (F) is zoomed in (E) near $r = 0.5cm$. In (E), the curves displayed from top to bottom are for J558-Ctrl tumor cells, J558-IL-27 tumor cells with small ($\alpha_{27} = 1.5 \times 10^{-5} pg/cell/day$), moderate ($\alpha_{27} = 7.5 \times 10^{-5} pg/cell/day$), and large ($\alpha_{27} = 3 \times 10^{-4} pg/cell/day$) production of IL-27, successively; $L = 1cm$.
doi:10.1371/journal.pone.0091844.g005

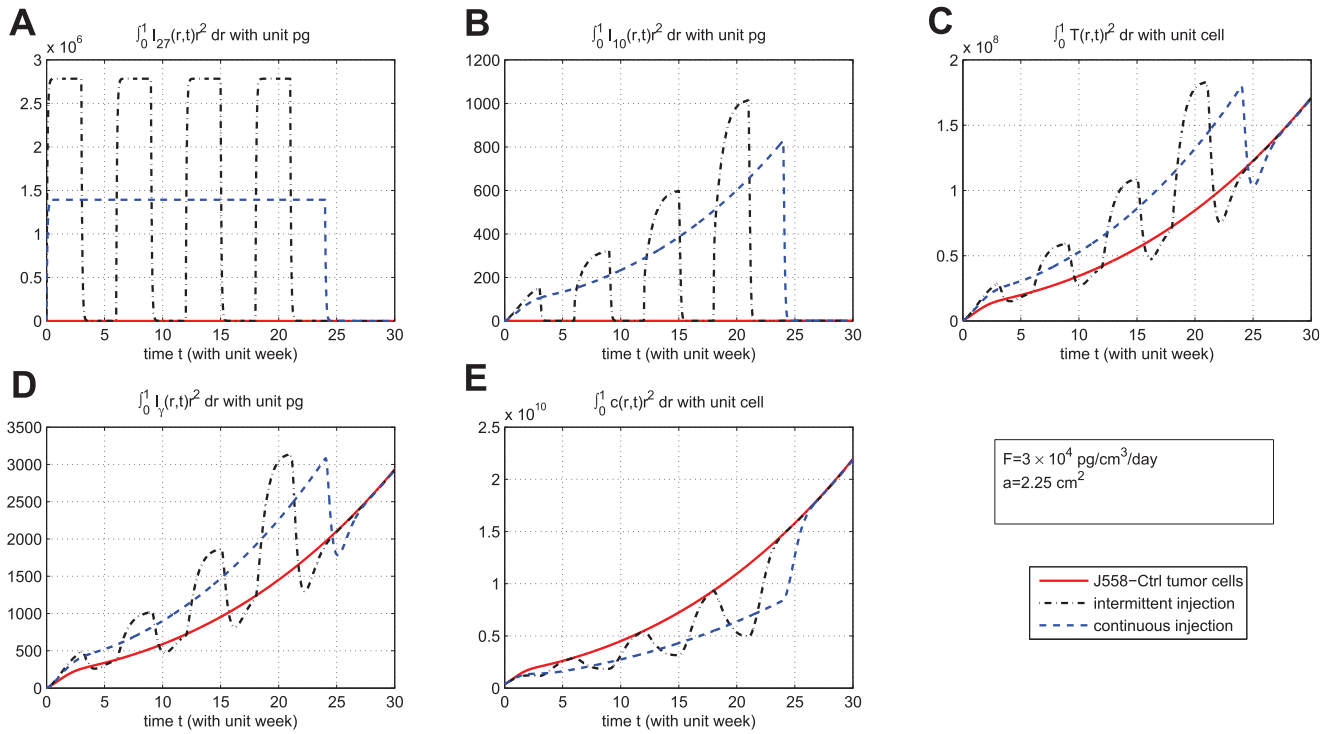

Figure 6. Comparison of continuous versus intermittent treatment. (A), (B), (C), (D), and (E) are the profiles of total number of $I_{27}, I_{10}, T, I_\gamma$, and c, respectively, for model (6) with $L=1.5cm$ which the first equation for I_{27} is replaced by (7) and all parameter values are taken from Table 6. In (E), the upper curve is for J558-Ctrl tumor cells, the dotted-dashed curve $(-\cdot-\cdot-)$ is for intermittent injection, and the dashed curve is for continuous injection with $F=3\times10^4 pg/cm^3/day$ and $a=2.25cm^2$, for the first 24 weeks.
doi:10.1371/journal.pone.0091844.g006

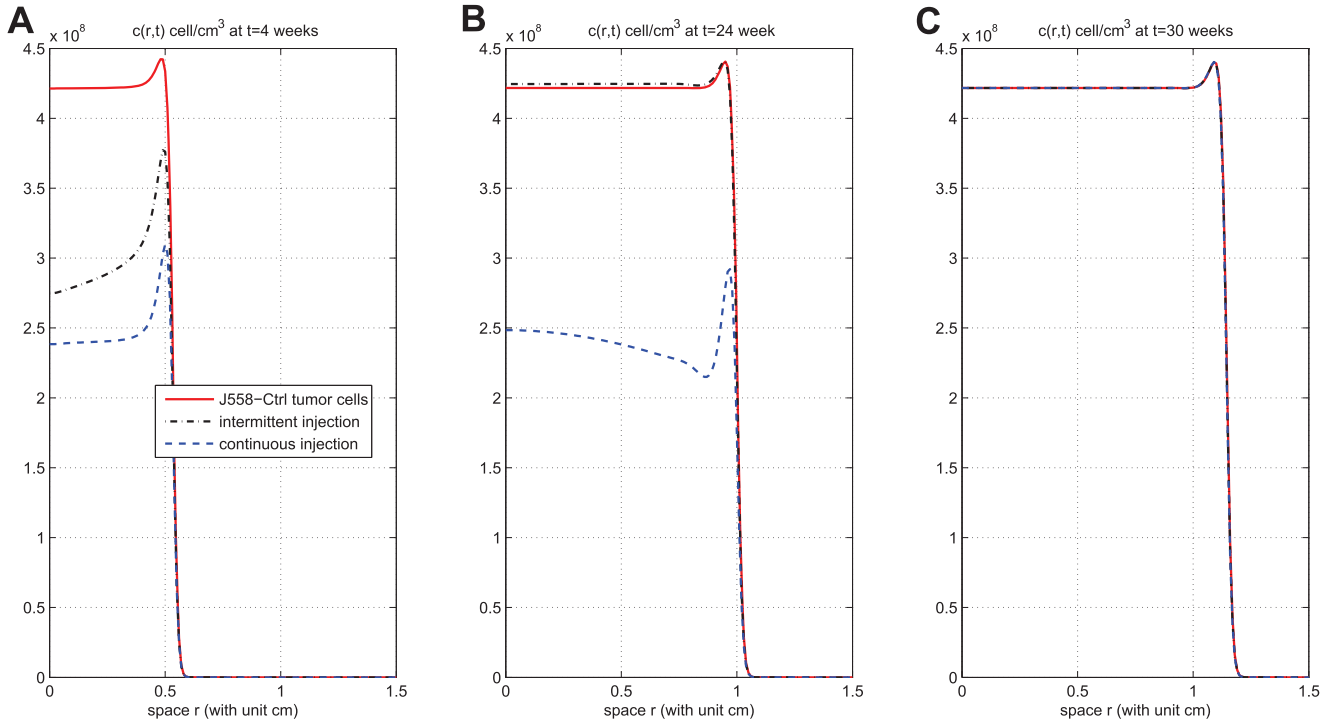

Figure 7. Concentration profiles of tumor cells at different times. (A), (B), and (C) are the concentration profiles of c at times 4 weeks (short time), 24 weeks (time at which injections are withdrew), and 30 weeks (the final time for simulation), respectively, under drug amount $F=3\times10^4 pg/cm^3/day$ and $a=2.25cm^2$. The upper curve is for J558-Ctrl tumor cells, the dotted-dashed curve $(-\cdot-\cdot-)$ is for intermittent injection, and the dashed curve is for continuous injection. The concentration of tumor cells are not visible, when r is close to $1.5cm$, for all $t\in[0,30weeks]$; $L=1.5cm$.
doi:10.1371/journal.pone.0091844.g007

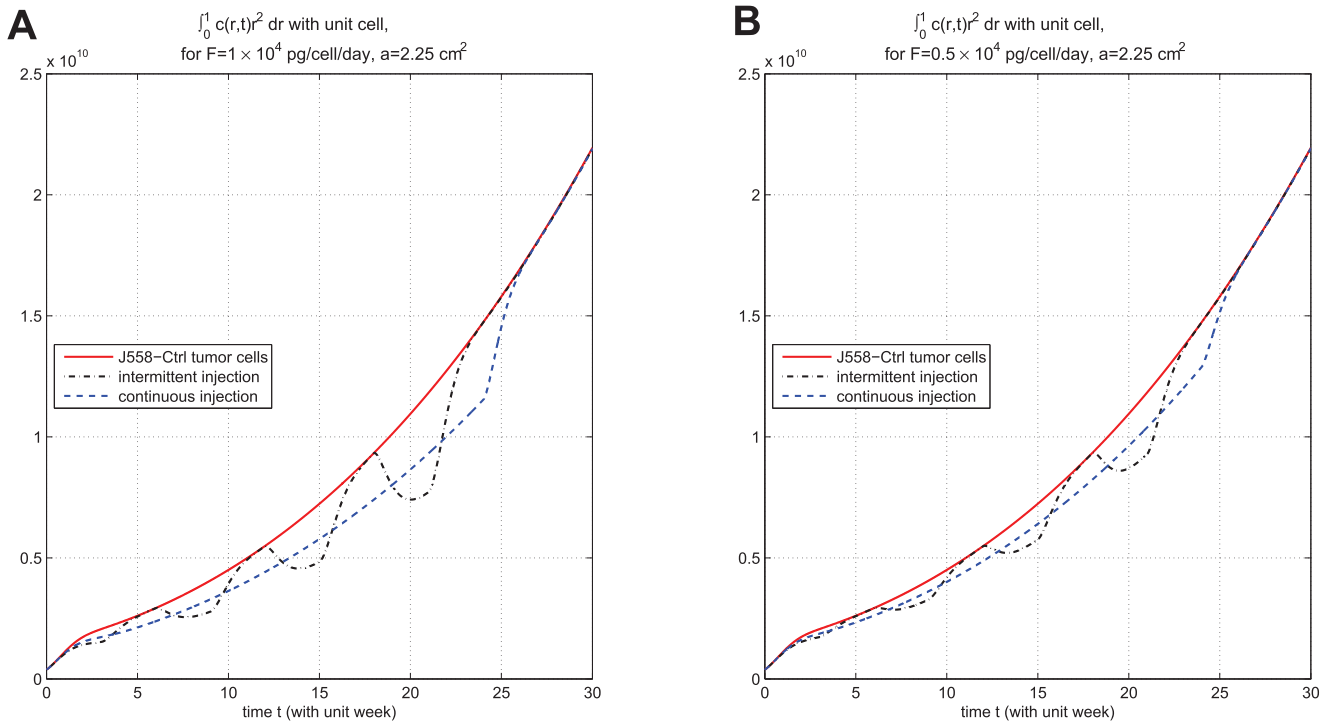

Figure 8. Comparison of continuous versus intermittent treatment for different drug amount. (A) and (B) are the profiles of total number of c with $F=1\times10^4 pg/cm^3/day$ and $F=0.5\times10^4 pg/cm^3/day$, respectively, for model (6) with $L=1.5cm$ and $a=2.25cm^2$ which the first equation for I_{27} is replaced by (7) and all parameter values are taken from Table 6. The upper curve is for J558-Ctrl tumor cells, the dotted-dashed curve $(-\cdot-\cdot-)$ is for intermittent injection, and the dashed curve is for continuous injection.
doi:10.1371/journal.pone.0091844.g008

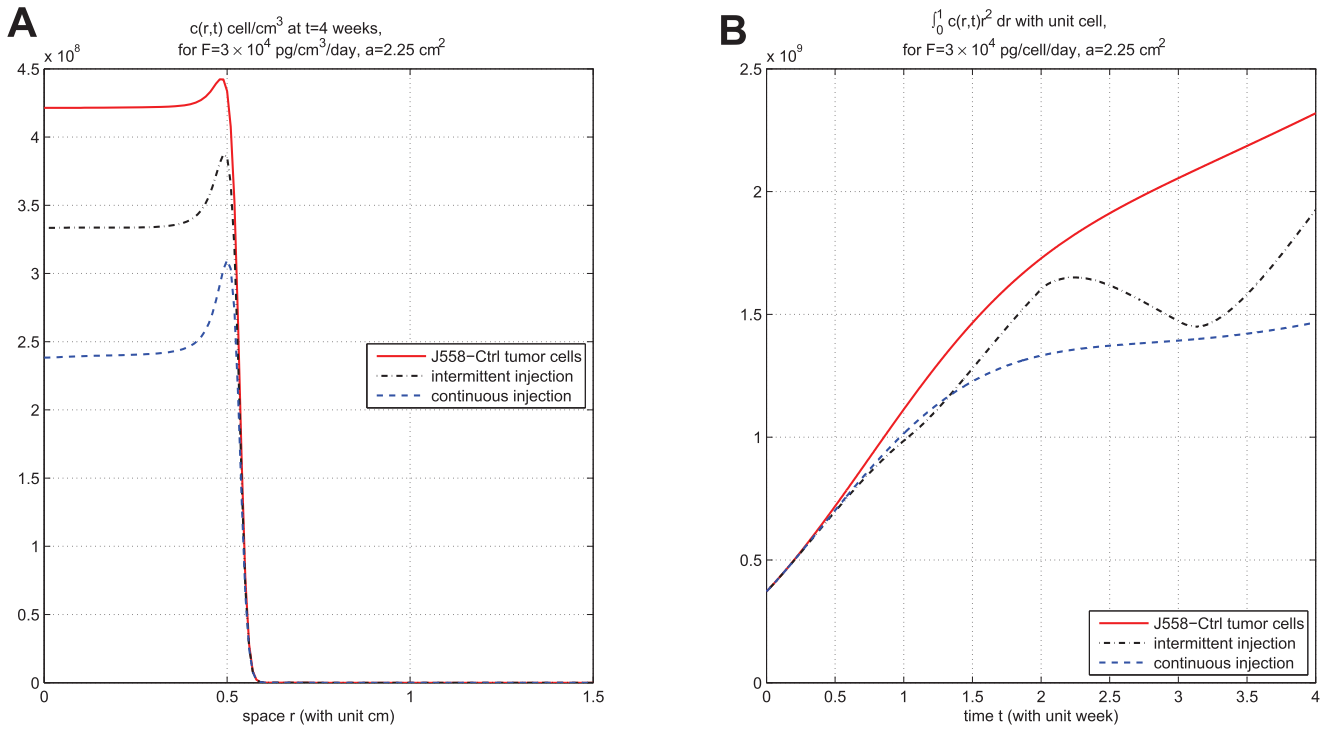

Figure 9. Tumor growth and migration for shorter injection schedule. (A) is the concentration profile of c at 4 weeks and (B) is the profile of total number of c for $t\in[0,4weeks]$, under $F=3\times10^4 pg/cm^3/day$, for model (6) with $L=1.5cm$ and $a=2.25cm^2$ which the first equation for I_{27} is replaced by (7) and all parameter values are taken from Table 6. The upper curve is for J558-Ctrl tumor cells, the dotted-dashed curve $(-\cdot-\cdot-)$ is for intermittent injection, and the dashed curve is for continuous injection. (A) shows that the concentration of tumor cells are not visible near the boundary $r=1.5cm$, for all $t\in[0,4weeks]$.
doi:10.1371/journal.pone.0091844.g009

Figure 7, for the same experiment as in Figure 6, shows the concentration profiles of tumor cells at times 4 weeks, 24 weeks, and 30 weeks for J558-Ctrl, intermittent injection, and continuous injection cases. Notice from Figures 7A, 7B, and 7C that the tumor has progressed during the periods of 4 weeks, 24 weeks, and 30 weeks to $r=0.6cm$, $r=1.05cm$, and $r=1.2cm$, respectively. Figures 6 and 7 show that I_{27} injection slows down tumor growth during drug injection, but it does not change the migration speed of tumor cells. Figure 8 compares the results of the above two strategies for smaller values of F, namely, $F=1\times10^4 pg/cm^3/day$ and $F=0.5\times10^4 pg/cm^3/day$. We see that continuous injection is still more effective, but, for smaller amount of injection, the relative advantage of continuous injection is decreased. Simulations of these two strategies for other values of F in the range of $10^3-10^6 pg/cm^3/day$ (not shown here) give the same results, namely, that continuous injection is preferable to intermittent injections. In order to make a definite recommendation on continuous versus intermittent injection one would need to consider also possible side-effects that may arise from these two strategies.

Although the expected lifespan of the mouse in the experiments of Liu et al. [30] was one month, for the purpose of therapy we performed simulations for the longer period of 30 weeks. But it is also interesting to consider the case of treatment for one month only. This is done in Figure 9 where we have taken in Equation (9) $0\le t\le4$ weeks for the continuous treatment, and, in Equation (10), intermittent time $t_j=j$ weeks. Figure 9 shows that continuous treatment is again preferable to intermittent treatment. Figure 9A shows the concentration profile of tumor cells at 4 weeks; note that tumor cells do not reach the boundary within 4 weeks. Figure 9B displays the profile of total number of tumor cells. We see that the continuous treatment still has better efficacy than intermittent treatment.

Sensitivity analysis

In order to provide support to the robustness of the simulation results, we ran sensitivity analysis on parameters which appear in Equations (1) – (5). The parameters chosen for the sensitivity analysis are either those whose baseline was crudely estimated, or those that seem to play more important role in the model predictions.

We list these parameters with their ranges, baselines, and units, in Table 7. In this analysis, $\hat{\alpha}_{27}$ varies from 32.4 to 12960. Following the sensitivity analysis method described in [43], we performed Latin hypercube sampling and generated 5000 samples to calculate the partial rank correlation coefficients (PRCC) and p-value, with respect to the ratio $\int_0^2 \hat{c}(\hat{r},\hat{t})\hat{r}^2d\hat{r}/\int_0^2 \hat{c}^-(\hat{r},\hat{t})\hat{r}^2d\hat{r}$, where $\hat{c}(\hat{r},\hat{t})$ (resp. $\hat{c}^-(\hat{r},\hat{t})$) accounts for the J558-IL27 (resp. J558-Ctrl) tumor cell density, at $\hat{t}=30$ and $\hat{r}\in[0,2]$. The PRCC and their p-values are listed in Table 8. A negative PRCC (i.e. negative correlation) means increase in the parameter value will decrease the ratio $\int_0^2 \hat{c}(\hat{r},\hat{t})\hat{r}^2d\hat{r}/\int_0^2 \hat{c}^-(\hat{r},\hat{t})\hat{r}^2d\hat{r}$; that is, it will increase the rejection of tumor treated by IL-27 versus untreated tumor. Conversely, positive PRCC means that increased rejection of the tumor (treated by IL-27 versus untreated) will occur if this parameter is decreased.

The sensitivity analysis data are shown in Figures S1–S4 in Supplementary Material and summarized in Table 8. The most significant negatively correlated parameters in promoting rejection of tumor treated by IL-27 versus untreated tumor are α_{27},σ_T,s_T; less significant parameters are $\eta_\gamma,\eta_c,\alpha_{10},\beta_T$. The effect of α_{27} has already been displayed in Figures 2–5. The negative correlations of s_T, η_c, and η_γ are not surprising, since s_T is the rate by which tumor activates T cells (while T cells are increased with IL-27 treatment; see Figures 2–5) and η_c and η_γ are, respectively, the killing rates of tumor cells by I_{10} and I_γ (while I_{10} and I_γ increase with IL-27 treatment; see Figures 2–5). The negative correlations of α_{10},σ_T, and β_T are also not surprising, since I_{27} promotes the production of I_{10} to inhibit tumor cells, and larger σ_T and β_T promote survival of $CD8^+$ T cells.

The most significant parameters in promoting tumor are σ_c,c_T,s_c and, to a smaller degree, σ_{10}. This also is not surprising, since increasing σ_c results in decreased inhibition of tumor cells by I_{10}, increasing c_T results in decreased number of $CD8^+$ T cells, increasing s_c results in decreased inhibition of tumor cells by I_γ, and increasing σ_{10} results in decreased I_{10}. We note that the parameters s_{10} and s_γ, in Table 8, have small PRCC with p-values that are larger than 0.01; this means that they are not sensitive to the ratio $\int_0^2 \hat{c}(\hat{r},\hat{t})\hat{r}^2d\hat{r}/\int_0^2 \hat{c}^-(\hat{r},\hat{t})\hat{r}^2d\hat{r}$.

Table 7. Parameters chosen for sensitivity analysis.

Parameter	Range	Baseline	Unit
$\hat{\alpha}_{27}$	$[3.24\times10,1.296\times10^4]$	3.24×10^2	pg/cell/day
$\hat{s}_{10}$	$[1.3335\times10^{-4},5.334\times10^{-4}]$	2.667×10^{-4}	pg/cell/day
$\hat{\alpha}_{10}$	$[1.692\times10^{-1},6.768\times10^{-1}]$	3.384×10^{-1}	pg/cell/day
$\hat{s}_T$	$[2.0952\times10^3,8.3808\times10^3]$	4.1904×10^3	cell/cm^3/day
$\hat{\sigma}_{10}$	$[2.5\times10,10^2]$	5×10	pg/cm^3
$\hat{\eta}_c$	$[5.175\times10^{-1},2.07]$	1.035	/day
$\hat{\eta}_\gamma$	$[9\times10^{-1},3.6]$	1.8	/day
$\hat{\sigma}_c$	$[1.5\times10^{-1},1.5\times10]$	1.5	pg/cm^3
$\hat{s}_c$	$[3\times10^{-1},3\times10]$	3	pg/cm^3
$\hat{s}_\gamma$	$[2.5\times10^4,10^5]$	5×10^4	pg/cm^3
$\hat{\sigma}_T$	$[2\times10^{-3},2\times10^{-1}]$	2×10^{-2}	pg/cm^3
$\hat{\beta}_T$	$[9\times10^{-1},9\times10]$	9	nondimension
$\hat{c}_T$	$[4\times10,1.6\times10^2]$	8×10	cell/cm^3

doi:10.1371/journal.pone.0091844.t007

Table 8. The PRCC and p-value of parameters for sensitivity analysis.

Parameter	PRCC	p-value
$\hat{\alpha}_{27}$	−0.63709	<0.01
$\hat{s}_{10}$	0.0074315	0.59933
$\hat{\alpha}_{10}$	−0.29952	<0.01
$\hat{s}_T$	−0.52728	<0.01
$\hat{\sigma}_{10}$	0.066589	<0.01
$\hat{\eta}_c$	−0.30727	<0.01
$\hat{\eta}_\gamma$	−0.38691	<0.01
$\hat{\sigma}_c$	0.53508	<0.01
$\hat{s}_c$	0.49864	<0.01
$\hat{s}_\gamma$	0.010033	0.47817
$\hat{\sigma}_T$	−0.59115	<0.01
$\hat{\beta}_T$	−0.10923	<0.01
$\hat{c}_T$	0.52848	<0.01

doi:10.1371/journal.pone.0091844.t008

Discussion

IL-12 plays a central role in linking the innate resistance and adaptive immunity, and could be a powerful anti-tumor agent. However, since IL-12 is excessively toxic, the cytokine IL-27, which is a less toxic member of the IL-12 family, has been considered as a possible replacement of IL-12 as anti-tumor agent [7,8,14–17]. It was demonstrated by Liu et al. [30] that IL-27 enhances the survival of tumor antigen specific $CD8^+$ T cells and induces their upregulation of IL-10, which acts as an anti-tumor cytokine. This suggests that IL-27 could play an important role in immunotherapy against human cancer.

The aim of the present paper was to develop a mathematical model that can be used to explore and predict the efficacy of different protocols of IL-27 treatment. To do that we first set up a dynamical system of partial differential equations whereby IL-27 is produced by transfected J558-IL-27 tumor cells, as demonstrated in the experiments of Liu et al. [30]. The model included IL-27-induced $CD8^+$ T cells and cytokines IL-10 and IFN-γ. By carefully estimating the parameters of the equations we showed that the model simulations agree with the experimental data of Liu et al. [30].

The model can be used to examine the effect of injecting IL-27 into the microenvironment of cancer in a mouse, and design strategies for such injections. We illustrated this by comparing the efficacy of two protocols: (i) continuous injection (e.g., daily) of IL-27 for 24 weeks at a fixed amount F, and (ii) intermittent injections during the first 24 weeks with three weeks injection at a fixed amount $2F$ followed by three weeks spacing, and withdrawing the drug after the 24 weeks for both protocols (i) and (ii). We found that the continuous injection has better efficacy in reducing the tumor load, and also in delaying relapse after the drug is withdrawn, while the treatment is ongoing. However, in establishing these results we made the assumption that IL-10 produced by IL-27 activated $CD4^+$ T cells has the same pro-inflammatory property as the IL-10 produced by $CD8^+$ T cells. In addition, we made the pharmacokinetic assumption that the drug density decreases toward the inner core of the tumor, and we also took the drug "amount" F in the range of $10^3-10^6 pg/cm^3/day$.

We note that our model was based on the experiments by Liu et al. [30] with plasmacytoma, but not with other tumor cells. Furthermore, the model did not include the effects of lymphoid and vascular compartments, as these were not reported in [30]. Hence the present paper should be considered only as an initial building block for a more comprehensive model which should include angiogenesis as well as the immune response of macrophages, dendritic cells, and T cells (Th1, Th2, Th17, and T_{reg}s). We note in particular that pro-inflammatory macrophages (M_1) secrete a family of IL-12 cytokines including IL-27 [44], and the IL-12 family attracts CTLs which kill tumor cells, so that M_1 macrophages suppress tumor growth. On the other hand, anti-inflammatory macrophages (M_2) secrete IL-10 which promotes tumor growth [23,24]. Regulatory T cells promote tumor growth and are inhibited by IL-27 [45,46]. Thus the present paper's prediction of the efficacy of different protocols of treatment of plasmacytoma in bone or soft tissue with IL-27 will need to be re-examined when more data become available that will enable us to include the important compartments of the immune and vascular systems.

We note also that the proposed intervention with IL-27 in our paper shows benefits only while the treatment is ongoing. The treatment has neither significant short-term benefits nor any long-term benefits after the drug has discontinued. It is becoming increasingly common to treat tumors with several drugs. In addition to tumor specific drugs, a generic mitotic inhibitory drug, which disrupts microtubules that pull the cell apart, is often used – since cancer cells are more sensitive to inhibition of mitosis than normal healthy cells. In our model, the effect of such a drug is to increase the death rate parameter in the equation for cancer cells. Further work should also include the combined effect of treatment of IL-27 with a mitotic inhibitory drugs.

Methods

Estimates of the densities of tumor cells and T cells

Many of the parameters are based on experiments reported in [30]. In [30], the volume of the tumor was measured in days 12,14,16, and 18, but the number of $CD8^+$ T cells and concentrations of I_{10} and I_γ were measured only in the first 5 days.

From Figure 5D in [30], the volume of the tumor at days 12,14,16, and 18 were approximate 30,60,100, and 180 in mm^3. Hence,

$$\begin{aligned} c(12) &= 30\times A, \quad c(14) = 60\times A,\\ c(16) &= 100\times A, \quad c(18) = 180\times A, \end{aligned} \tag{11}$$

where A is the number of tumor cells in per mm^3. If we consider a simplified equation for (5)

$$\frac{dc(t)}{dt} = \lambda_1 c(t) - \mu_c c(t),$$

then, for any two times t_1 and t_2,

$$c(t_2) = c(t_1)e^{(\lambda_1-\mu_c)(t_2-t_1)}.$$

If we apply this formula to the 6 pairs of the numbers from (11) to compute $\lambda_1-\mu_c$ and take the mean value, we get

$$\lambda_1-\mu_c = 0.295/day.$$

Since the half-life of melanoma tumor cells is approximate 4 days, [47],

$$\mu_c = ln2/4/day \approx 0.173/day,$$

and then $\lambda_1 = 0.468/day$.

In the experiments in [30], there were two kinds of tumor cells: J558-IL-27 which generates IL-27, and J558-Ctrl which does not generate IL-27. The antigen P1A on J558 tumor cells is recognized by receptors TCRs on cytotoxic T cells, P1CTL. Liu et al. [30] used P1CTL with glycoprotein CD8 (which is called $CD8^+$ T cells) to investigate the immune response for IL-27. Their P1CTL cells were of four different types: (i) P1CTL which can recognize J558-Ctrl tumor cells and generate IL-10 to inhibit tumor growth; (ii) $IL\text{-}10^{-/-}$P1CTL which can recognize J558-Ctrl tumor cells but cannot generate IL-10; (iii) P1CTL/IL-27 which can recognize J558-IL-27 tumor cells and generate IL-10; and (iv) $IL\text{-}10^{-/-}$P1CTL/IL-27 which can recognize J558-IL-27 tumor cells but cannot generate IL-10.

The number of tumor cells at $t=0$ day (in [30]) was 5×10^6 cells, and we assume (see Figure 5D in [30]) that they occupy volume $10mm^3$. Hence

$$c(0)=5\times10^{8}cell/cm^{3}. \tag{12}$$

There is no data in [30] on the density of the tumor in day 5. We assume that this density is larger than $c(0)$ but substantively smaller than the maximal capacity $10^{9}cell/cm^{3}$. We take

$$c(5)=5.05\times10^{8}cell/cm^{3}, \tag{13}$$

for J558-Ctrl with P1CTL or J558-IL-27 with P1CTL/IL-27, but

$$c(5)=5.1\times10^{8}cell/cm^{3}, \tag{14}$$

for J558-Ctrl with IL-$10^{-/-}$P1CTL or J558-IL-27 with IL-$10^{-/-}$P1CTL/IL-27, since the last two types of T cells do not generate I_{10}.

From Figure 1A in [30], there were 1.1×10^{6} P1CTL at day 1 and 2.6×10^{6} P1CTL at day 5; 10^{6} P1CTL/IL-27 at day 1 and 5×10^{6} P1CTL/IL-27 at day 5. We assume that these $CD8^{+}$ T cells occupy the volume of $10mm^{3}$ for the first 5 days. Hence

$$T(1)=1.1\times10^{8}cell/cm^{3},T(5)=2.6\times10^{8}cell/cm^{3},\quad \text{for P1CTL} \tag{15}$$

$$T(1)=10^{8}cell/cm^{3},T(5)=5\times10^{8}cell/cm^{3},\quad \text{for P1CTL/IL-27}. \tag{16}$$

Estimate of the parameters in (1)

Since IL-27 belongs to the IL-12 family, we take its diffusion coefficient and the degradation rate to be the same as for IL-12 [48]:

$$D_{I_{27}}=1.25\times10^{-3}cm^{2}/day,$$

$$\mu_{27}=2/day.$$

In order to find α_{27}, we use the simplified version of Equation (1):

$$\frac{dI_{27}(t)}{dt}=\alpha_{27}c-\mu_{27}I_{27}(t).$$

If c is taken to be a constant, then

$$I_{27}(5)=e^{-5\mu_{27}}I_{27}(0)+\frac{\alpha_{27}c}{\mu_{27}}(1-e^{-5\mu_{27}}). \tag{17}$$

From Figure 1A in [30], $I_{27}(0)=5\times10^{4}pg/cm^{3}$ and only $5-10\%$ of I_{27} remained in day 5. We assume that 7.5% of I_{27} remained at day 5, so that

$$I_{27}(0)=5\times10^{4}pg/cm^{3}\ \text{and}\ I_{27}(5)=3750pg/cm^{3}. \tag{18}$$

Taking c to be the average between the values at days 0 and 5 (see (12) and (13)) and recalling (17), we get

$$3750pg/cm^{3}=e^{-5day\times2/day}\times5\times10^{4}pg/cm^{3}+\frac{\alpha_{27}}{2/day}\times(5.025\times10^{8})cell/cm^{3}\times(1-e^{-5day\times2/day}),$$

so that $\alpha_{27}=1.5\times10^{-5}pg/cell/day$

.

Estimate of the parameters in (2)

We consider a simplified version of Equation (2):

$$\frac{dI_{10}(t)}{dt}=s_{10}T+\alpha_{10}T\frac{I_{27}}{I_{27}+\sigma_{10}}-\mu_{10}I_{10}(t). \tag{19}$$

From [48], we have $\mu_{10}=16/day$. To estimate s_{10}, we consider the case of J558-Ctrl tumor cells, for which the term with I_{27} is removed from (19):

$$\frac{dI_{10}(t)}{dt}=s_{10}T-\mu_{10}I_{10}(t).$$

If T is constant, then

$$I_{10}(5)=e^{-4\mu_{10}}I_{10}(1)+\frac{s_{10}T}{\mu_{10}}(1-e^{-4\mu_{10}}).$$

From the profile of P1CTL in Figure 3D of [30], we have $I_{10}(1)=300pg/cm^{3}$ at day 1 and $I_{10}(5)=1pg/cm^{3}$ at day 5 and we take T to be the mean value of $T(1)$ and $T(5)$ in (15). We then get

$$1pg/cm^{3}=e^{-4day\times16/day}\times300pg/cm^{3}+\frac{s_{10}\times1.8\times10^{8}cell/cm^{3}}{16/day}\times(1-e^{-4day\times16/day}),$$

so that $s_{10}=8.89\times10^{-8}pg/cell/day$.

Next, we choose $\sigma_{10}=5\times10^{3}pg/cm^{3}$ and proceed to compute α_{10}. We then consider J558-IL-27 tumor cells which can generate I_{27}. For simplicity, we take T to be the average between the values at days 1 and 5 (see (16)) and I_{27} to be the average between the values at days 0 and 5 (see (18):

$$T=3\times10^{8}cell/cm^{3}\ \text{and}\ I_{27}=26875pg/cm^{3}.$$

Then, the solution of Equation (19) satisfies

$$I_{10}(5)=e^{-4\mu_{10}}I_{10}(1)+\frac{1}{\mu_{10}}(s_{10}T+\alpha_{10}T\frac{I_{27}}{I_{27}+\sigma_{10}})(1-e^{-4\mu_{10}}).$$

From the profile of P1CTL/IL-27 in Figure 3D of [30], we have $I_{10}(1)=400pg/cm^3$ at day 1 and $I_{10}(5)=1800pg/cm^3$ at day 5, so that

$$\begin{aligned}1800pg/cm^3=&e^{-4day\times 16/day}\times 400pg/cm^3\\&+\frac{1}{16/day}[8.89\times 10^{-8}\times 3\times 10^8\\&+\alpha_{10}\times 3\times 10^8\\&\times\frac{26875pg/cm^3}{26875pg/cm^3+5000pg/cm^3}](1-e^{-4day\times 16/day}).\end{aligned}$$

Therefore, we take $\alpha_{10}=1.128\times 10^{-4}pg/cell/day$.

Estimate of the parameters in (3)

From [48], we have $\mu_T=0.3/day$. For J558-Ctrl tumor cells, the term of I_{27} in (3) drops out, and we consider a simplified version:

$$\frac{dT(t)}{dt}=s_T\frac{c}{c+c_T}-\mu_T T(t),$$

which, if c is constant, has the solution

$$T(5)=e^{-4\mu_T}T(1)+\frac{s_T c}{\mu_T(c+c_T)}(1-e^{-4\mu_T}).$$

Substituting $T(1)$ and $T(5)$ from (15), we get

$$2.6\times 10^8 cell/cm^3-e^{-4day\times 0.3/day}\times 1.1\times 10^8 cell/cm^3 \quad (20)$$

$$=\frac{s_T}{\mu_T}\times\frac{c}{c+c_T}\times(1-e^{-4day\times 0.3/day}). \quad (21)$$

Based on the fact that the (20) is close to 2.3×10^8 while the (16) is close to $2.3s_T\frac{c}{c+c_T}$, we choose $s_T=1.3968\times 10^8 cell/cm^3/day$.

Next, we consider

$$\frac{dT(t)}{dt}=s_T\frac{c}{c+c_T}-\frac{\mu_T}{1+\sigma_T I_{27}+\beta_T\sigma_T I_{10}}T(t)$$

where the solution satisfies

$$T(5)=e^{-4w_T}T(1)+\frac{s_T c}{w_T(c+c_T)}(1-e^{-4w_T})$$

with $w_T=\frac{\mu_T}{1+\sigma_T I_{27}+\beta_T\sigma_T I_{10}}$. Recalling $T(1)$ and $T(5)$ from (16), we get

$$\begin{aligned}(5-e^{-4w_T})\times 10^8 cell/cm^3=&\frac{1.3968\times 10^8}{w_T}\\&\times(1-e^{-4w_T})\times\frac{c}{c+c_T}.\end{aligned} \quad (22)$$

In (22), the left-hand side is close to 5×10^8 and the right-hand side is close to $5.52\times\frac{c}{c+c_T}\times 10^8$, while we take $\sigma_T=2\times 10^{-4}pg/cm^3$ and $\beta_T=9$.

Estimate of the parameters in (4)

We assume that the diffusion coefficient of I_γ is the same as that of I_{27}, namely, $D_\gamma=1.25\times 10^{-3}cm^2/day$. Next we use the simplified version:

$$\frac{dI_\gamma(t)}{dt}=\alpha_\gamma T\frac{s_\gamma}{s_\gamma+I_{27}}-\mu_\gamma I_\gamma(t), \quad (23)$$

where $\mu_\gamma=2.16/day$ by [49]. For tumor cells J558-Ctrl (which do not generate I_{27}), (23) reduces to

$$\frac{dI_\gamma(t)}{dt}=\alpha_\gamma T-\mu_\gamma I_\gamma(t). \quad (24)$$

If T is constant, then the solution of (24) satisfies

$$I_\gamma(5)=e^{-4\mu_\gamma}I_\gamma(1)+\frac{\alpha_\gamma T}{\mu_\gamma}(1-e^{-4\mu_\gamma}).$$

Taking T to be the average of $T(1)$ and $T(5)$ in (15) and taking $I_\gamma(t)$ from the curve P1CTL in the right part of Figure 3D in [30], we have

$$\begin{aligned}3100pg/cm^3=&e^{-4day\times 2.16/day}\times 250pg/cm^3\\&+\frac{\alpha_\gamma\times 1.8\times 10^8 cell/cm^3}{2.16/day}\times(1-e^{-4day\times 2.16/day})\end{aligned}$$

so that $\alpha_\gamma=3.72\times 10^{-5}pg/cell/day$. We choose $s_\gamma=5\times 10^6 pg/cm^3$.

Estimate of the parameters in (5)

We consider a simplified version of (5):

$$\frac{dc(t)}{dt}=\lambda_1 c(t)-\mu_c c(t)-\eta_c\frac{I_{10}}{I_{10}+\sigma_c}c(t)-\eta_\gamma\frac{I_\gamma}{I_\gamma+s_c}c(t). \quad (25)$$

We choose $s_c=300pg/cm^3$. In order to compute η_γ, we consider T cells IL-$10^{-/-}$P1CTL and IL-$10^{-/-}$P1CTL/IL-27 which do not generate I_{10}, so that I_{10} drops out of Equation (25):

$$\frac{dc(t)}{dt}=\lambda_1 c(t)-\mu_c c(t)-\eta_\gamma\frac{I_\gamma}{I_\gamma+s_c}c(t).$$

If I_γ is constant, then the solution is $c(t)=e^{(\lambda_1-\mu_c-\eta_\gamma\frac{I_\gamma}{I_\gamma+s_c})t}c(0)$ which leads to

$$\eta_\gamma=[(\lambda_1-\mu_c)-\frac{1}{t}\ln\frac{c(t)}{c(0)}]\times\frac{I_\gamma+s_c}{I_\gamma}. \quad (26)$$

Since $c(5)/c(0)$ is close to 1 and the range of I_γ may vary from $100pg/cm^3$ to $3400pg/cm^3$ forJ558-Ctrl tumor cells and IL-$10^{-/-}$P1CTL T cells or from $750pg/cm^3$ to $1600pg/cm^3$ for J558-IL27 tumor cells and IL-$10^{-/-}$P1CTL/IL27, we choose in Equation (26)

$$\frac{I_\gamma+s_c}{I_\gamma}\approx 2.$$

Recalling that $\lambda_1-\mu_c=0.295/day$, we take $\eta_\gamma=0.6/day$.

Next, we choose $\sigma_c=150pg/cm^3$ and proceed to estimate η_c by considering T cells P1CTL and P1CTL/IL-27 which generate I_{10}. For (25), if I_{10} and I_γ are constants, then the solution is $c(t)=e^{(\lambda_1-\mu_c-\eta_c\frac{I_{10}}{I_{10}+\sigma_c}-\eta_\gamma\frac{I_\gamma}{I_\gamma+s_c})t}c(0)$, and hence

$$\eta_c=[\lambda_1-\mu_c-\eta_\gamma\frac{I_\gamma}{I_\gamma+s_c}-\frac{1}{t}\ln\frac{c(t)}{c(0)}]\times\frac{I_{10}+\sigma_c}{I_{10}}/day$$

$$\approx(0.295/day-0.6/day\times\frac{I_\gamma}{I_\gamma+s_c})\times\frac{I_{10}+\sigma_c}{I_{10}}.$$

The concentration of I_γ with I_{10} is smaller than the concentration of I_γ where I_{10} is blocked [30]. We take $\frac{I_\gamma}{I_\gamma+s_c}\approx\frac{1}{3}$. In [30], the concentration of I_{10} vary from $1pg/cm^3$ to $2500pg/cm^3$. We take $\sigma_c=150pg/cm^3$, so that $\frac{I_{10}+\sigma_c}{I_{10}}\approx 3.5$; hence $\eta_c=0.345/day$.

Supporting Information

Figure S1 Sensitivity analysis. Sensitivity analysis on α_{27},s_{10},α_{10}, and s_T.
(PDF)

Figure S2 Sensitivity analysis. Sensitivity analysis on σ_{10},η_c,η_γ, and σ_c.
(PDF)

Figure S3 Sensitivity analysis. Sensitivity analysis on s_c,s_γ,σ_T, and β_T.
(PDF)

Figure S4 Sensitivity analysis. Sensitivity analysis on c_T.
(PDF)

Author Contributions

Conceived and designed the experiments: KL XB AF. Performed the experiments: KL XB AF. Analyzed the data: KL XB AF. Contributed reagents/materials/analysis tools: KL XB AF. Wrote the paper: KL XB AF.

References

1. Brunda MJ, Luistro L, Warrier RR, Wright RB, Hubbard BR, et al. (1993) Antitumor and antimetastatic activity of interleukin 12 against murine tumors. The Journal of Experimental Medicine 178: 1223–1230.
2. Cavallo F, Giovarelli M, Forni G, Signorelli P, Musiani P, et al. (1997) Antitumor efficacy of adenocarcinoma cells engineered to produce interleukin 12 (il-12) or other cytokines compared with exogenous il-12. Journal of the National Cancer Institute 89: 1049–1058.
3. Colombo MP, Trinchieri G (2002) Interleukin-12 in anti-tumor immunity and immunotherapy. Cytokine Growth Factor Rev 13: 155–168.
4. Rakhmilevich AL, Janssen K, Turner J, Culp J, Yang NS (1997) Cytokine gene therapy of cancer using gene gun technology: superior antitumor activity of interleukin-12. Hum Gene Ther 8: 1303–1311.
5. Car BD, Eng VM, Lipman JM, Anderson TD (1999) The toxicology of interleukin-12: A review. Toxicologic Pathology 27: 58–63.
6. Marshall E (1995) Cancer trial of interleukin-12 halted. Science (Wash DC) 268: 1555.
7. Hisada M, Kamiya S, Fujita K, Belladonna ML, Aoki T, et al. (2004) Potent antitumor activity of interleukin-27. Cancer Res 64: 1152–1156.
8. Hall AO, Silver JS, Hunter CA (2012) The immunobiology of il-27. Adv Immunol 115: 1–44.
9. Murugaiyan G, Mittal A, Lopez-Diego R, Maier LM, Anderson DE, et al. (2009) Il-27 is a key regulator of il-10 and il-17 production by human cd4+ t cells. J Immunol 183: 2435–2443.
10. Stumhofer JS, Silver JS, Laurence A, Porrett PM, Harris TH, et al. (2007) Interleukins 27 and 6 induce stat3-mediated t cell production of interleukin 10. Nat Immunol 8: 1363–1371.
11. Swarbrick A, Junankar SR, Batten M (2013) Could the properties of il-27 make it an ideal adjuvant for anticancer immunotherapy? OncoImmunology 2:8: e25409.
12. Ho MY, Leu SJ, Sun G, Tao M, Tang SJ, et al. (2009) Il-27 directly restrains lung tumorigenicity by suppressing cyclooxygenase-2-mediated activities. J Immunol 183: 6217–6226.
13. Zolochevska O, Diaz-Quinönes AO, Ellis J, Figueiredo ML (2013) Interleukin-27 expression modifies prostate cancer cell crosstalk with bone and immune cells in citro. J Cell Physiol 228: 1127–1136.
14. Chiyo M, Shimozato O, Lizasa T, Fujisawa T, Tagawa M (2004) Antitumor effects produced by transduction of dendritic cells-derived heterodimeric cytokine genes in murine colon carcinoma cells. Anticancer Res 24: 3763–3767.
15. Salcedo R, Stauffer JK, Lincoln E, Back TC, Hixon JA, et al. (2004) Il-27 mediated complete regression of orthotopic promary and metastatic murine neuroblastoma tumors: role for cd8+ t cells. J Immunol 173: 7170–7182.
16. Salcedo R, Hixon JA, Stauffer JK, Jalah R, Brooks AD, et al. (2009) Immunologic and therapeu tic synergy of il-27 and il-2: ehancement of t cell sensitization, tumor-specific ctl reactivity and complete regression of disseminated neuroblastoma metastases in the liver and bone marrow. J Immunol 182: 4328–4338.
17. Zhu S, Lee DA, Li S (2010) Il-12 and il-27 sequential gene therapy via intramuscular eletroporation delivery for eliminating distal aggressive tumors. J Immunol 184: 2348–2354.
18. Morishima N, Mizoguchi I, Okumura M, Chiba Y, Shimizu M, et al. (2010) A prvotal role for interleukin-27 in cd8+ t cell functions and generation of cutotoxic t lymphocytes. J Biomed Biotechnol.
19. Shinozaki Y, Wang S, Miyazaki Y, Miyazaki K, Yamada H, et al. (2009) Tumor-specific cutotoxic t cell generation and dendritic cell function are differentially regulated by interleukin 27 during development of anti-tumor immunty. Int J Cancer 124: 1372–1378.
20. Groux H, Bigler M, Vries JE, Roncarolo MG (1998) Inhibitory and stimulatory effects of il-10 on human cd8 + t cells. J Immunol 160: 3188–3193.
21. Brooks DG, Walshb KB, Elsaessera H, Oldstone MBA (2010) Il-10 directly suppresses cd4 but not cd8 t cell effector and memory responses following acute viral infection. PNAS 107: 3018–3023.
22. Asadullah K, Sterry W, Volk HD (2003) Interleukin-10 therapy - review of a new approach. Phar macological Reviews 55: 241–269.
23. Wang R, Lu M, Zhang J, Chen S, Luo X, et al. (2011) Increased il-10 mrna expression in tumor associated macrophage correlated with late stage of lung cancer. Journal of Experimental & Clinical Cancer Research 30.
24. Itakura E, Huang RR, Wen DR, Paul E, Wünsch P, et al. (2011) Il-10 expression by primary tumor cells correlates with melanoma progression from radial to vertical growth phase and development of metastatic competence. Modern Pathology 24: 801–809.
25. Grous H, Coottrez F, Rouleau M, Mauze S, Antonenko S, et al. (1999) A transgenic model to analyze the immunoregulatory role of il-10 secreted by antigen-presenting cells. J Immunol 162: 1723–1729.
26. Mumm JB, Emmerich J, Zhang X, Chan I, Mauze L, et al. (2011) Il-10 elicits ifn-γ-dependent tumor immune surveillance. Cancer Cell 20: 781–796.

27. Tanikawa T, Wilke CM, Kryczek I, Chen GY, Kao J, et al. (2012) Interleukin-10 ablation promotes tumor development, growth and metastasis. Cancer Res 72: 420–429.
28. Fujii S, Shimizu K, Shimizu T, Lotze MT (2001) Interleukin-10 promotes the maintenance of antitumor cd8(+) t-cell effector function in situ. Blood 98: 2143–2151.
29. Batten M, Kljavin NM, Li J, Walter MJ, Sauvage FJd, et al. (2008) Cutting edge: Il-27 is a potent inducer if il-10 but nor foxp3 in murine t cells. J Immunol 180: 2752–2756.
30. Liu Z, Liu JQ, Talebian F, Wu LC, Li S, et al. (2013) Il-27 enhances the survival of tumor antigen specific cd8+ t cells and programs them into il-10-producing, memory precursor-like effector cells. European Journal of Immunology 43: 468–479.
31. Aguda BD, Friedman A (2008) Models of cellular regulation. Oxford graduate texts.
32. Bresch D, Colin T, Grenier E, Ribba B, Saut O (2010) Computation modeling of solid tumor growth: the avascular stage. SIAM J Scientific Computing 32: 2321–2344.
33. Byrne HM, Chaplain MAJ (1995) Growth of non-necrotic tumours in the presence and absence of inhibitors. Math Biosci 2: 151–181.
34. Chaplain MAJ, Deakin NE (2013) Mathematical modelling of cancer invasion: The role of membrane-bound matrix metalloproteinases. Frontiers in Oncology 3.
35. Chaplain MAJ, Lolas G (2006) Mathematical modelling of cancer invasion of tissue: dynamic heterogeneity. Networks and Heterogeneous Media 1: 399–439.
36. McGillen JB, Gaffney EA, Martin NK, Maini PK (2013) A general reaction-diffusion model of acidity in cancer invasion. J Math Biol.
37. Szomolay B, Eubank TD, Roberts RD, Marsh CB, Friedman A (2012) Modeling the inhibition of breast cancer growth by gm-csf. J Theore Biol 303: 141–151.
38. Szymańska Z, Rodrigo CM, Lachowicz M, Chaplain MAJ (2009) Mathematical modelling of cancer invasion of tissue: the role and effect of nonlocal interactions. Math Models Methods Appl Sci 19: 257–281.
39. Mocellin S, Marinola FM, Young HA (2005) Interleukin-10 and the immune response against cancer: a counterpoint. J Leukocyte Biology 78: 1043–1051.
40. Ikeda H, Old LJ, Schreiber RD (2002) The roles of ifn gamma in protection against tumor devel opment and cncer immunoediting. Cytokine & Growth Factor Reviews 13: 95–109.
41. Roth AD, Hornicek FJ, Gerstner CG, Kirkwood JM (1991) Effects of interferon-gamma and tu mor necrosis factor-alpha on the development of cytotoxic t lymphocytes in autologous mixed lymphocyte tumor cultures with human melanoma. Clin exp Immunol 86: 163–172.
42. Romanos MA, Scorer CA, Clare JJ (1992) Foregin gene expression in yeast: a review. Yeast 8: 423–488.
43. Marino S, Hogue IB, Ray CJ, Kirschner DE (2008) A methodology for performing global uncer taintly and sensitivity analysis in systems biology. J Theor Biol 254: 178–196.
44. Xu M, Mizoguchi I, Morishima N, Chiba Y, Mizuguchi J, et al. (2010) Regulation of antitumor immune responses by the il-12 family cytokines, il-12, il-23, and il-27. Clin Dev Immunol.
45. Huber M, Steinwald V, Guralnik A, Brüstle A, Kleemann P, et al. (2008) Il-27 inhibits the devel opment of regulatory t cells via stat3. International Immunology 20: 223–234.
46. Wojno ED, Hosken N, Stumhofer JS, O'Hara AC, Mauldin E, et al. (2011) A role for il-27 in limiting t regulatory cell populations. J Immunol 187: 266–273.
47. Lemech C, Arkenau HT (2012) Nocel treatments for metastatic cutaneous melanoma and the management of emergent toxicites. Clinical medicine insights: oncology 6: 53–66.
48. Liao KL, Bai XF, Friedman A (2013) The role of cd200-cd200r in tumor immune evasion. J Theor Biol 328: 65–76.
49. Day J, Friedman A, Schlesinger LS (2008) Modeling the immune rheostat of macrophages in the lung in response to infection. PNAS 106: 11246–11251.